International Journal of Solids and Structures 51 (2014) 3350–3360

Contents lists available at ScienceDirect

International Journal of Solids and Structures

journal homepage: www.elsevier.com/locate/ijsolstr

# A peridynamic implementation of crystal plasticity

S. Sun [1], V. Sundararaghavan *

*University of Michigan, 1320 Beal Ave, 3025 FXB Building, Ann Arbor, MI 48109, USA*

ARTICLE INFO

*Article history:*
Received 19 March 2014
Received in revised form 22 May 2014
Available online 19 June 2014

*Keywords:*
Microstructure
Crystal plasticity
Peridynamics
Simulation
Theory

ABSTRACT

This paper presents the first application of peridynamics theory for crystal plasticity simulations. A state-based theory of peridynamics is used (Silling et al., 2007) where the forces in the bonds between particles are computed from stress tensors obtained from crystal plasticity. The stress tensor at a particle, in turn, is computed from strains calculated by tracking the motion of surrounding particles. We have developed a quasi-static implementation of the peridynamics theory. The code employs an implicit iterative solution procedure similar to a non-linear finite element implementation. Peridynamics results are compared with crystal plasticity finite element (CPFE) analysis for the problem of plane strain compression of a planar polycrystal. The stress, strain field distribution and the texture formation predicted by CPFE and peridynamics were found to compare well. One particular feature of peridynamics is its ability to model fine shear bands that occur naturally in deforming polycrystalline aggregates. Peridynamics simulations are used to study the origin and evolution of these shear bands as a function of strain and slip geometry.


## 1. Introduction

Efficient micro-scale modeling tools are needed to compute microstructure-dependent properties of advanced structural alloys used in aerospace, naval and automotive applications. Integrated Computational Materials Engineering (ICME) (Allison et al., 2006) is an emerging paradigm that emphasizes integration of micro-scale material models with engineering analysis of products and processes so as to enable design of microstructurally tailored materials. One such model for metallic materials is based on finite element analysis of polycrystalline aggregates via crystal plasticity theory (Harren and Asaro, 1989; Bronkhorst et al., 1992; Becker and Panchanadeeswaran, 1995; Beaudoin et al., 1996; Sarma et al., 2002; Sundararaghavan and Zabaras, 2008). Here, mechanical properties of aggregates of grains are analyzed by discretizing the grains into finite elements and assigning crystallographic orientation to grains based on microdiffraction measurements (Qidwai et al., 2009). Deformation mechanisms are modeled using constitutive laws that consider crystallographic slip and reorientation of grains (texturing).

One particular drawback of standard finite element methods for crystal plasticity is observed during modeling of plastic localization zones. Such localization naturally occurs in deforming polycrystalline aggregates in the form of fine shear bands (Harren et al., 1988). The strains in these bands have been recently measured using micro-scale digital image correlation (DIC) (e.g. Kammers and Daly, 2013, see Fig. 1). In standard finite elements, the element size determines the size of shear bands (Anand and Kalidindi, 1994). Various enhancements of finite element method have been studied in the past to address the issue of mesh dependency. Early approaches involved development of traction-separation softening laws whose slope was made to depend on the element size (Oliver, 1989). In the limiting case of zero element size, the localization appears as a sharp discontinuity. Later approaches such as the extended finite element methods (X-FEM, Samaniego and Belytschko, 2005) or variational multiscale methods (VMM, Armero and Garikipati, 1996) directly represented discontinuities on coarse elements by enriching the finite element interpolations using fine-scale strain functions.

Another approach employs models that possess an intrinsic characteristic length scale. Examples of these ideas are non-local constitutive models (Bazant et al., 1984; Ghosh et al., 2013, 2014; Sundararaghavan and Waas, 2011), higher-gradient models (Coleman and Hodgdon, 1987) and more recently, peridynamic models (Silling, 2000). In peridynamics, the continuum domain is represented as a set of interacting particles. A state-based theory of peridynamics developed in Silling et al. (2007) formulates the forces between particles based on stress tensors obtained from continuum formulations (e.g. crystal plasticity). The stress tensor at a particle, in turn, is computed from strains calculated by tracking

* Corresponding author. Address: Associate Professor, Department of Aerospace Engineering. Tel.: +1 734 615 7242.
*E-mail addresses:* shangsun@umich.edu (S. Sun), veeras@umich.edu (V. Sundararaghavan).
[1] PhD Candidate, Department of Naval Architecture and Marine Engineering.

http://dx.doi.org/10.1016/j.ijsolstr.2014.05.027
0020-7683/

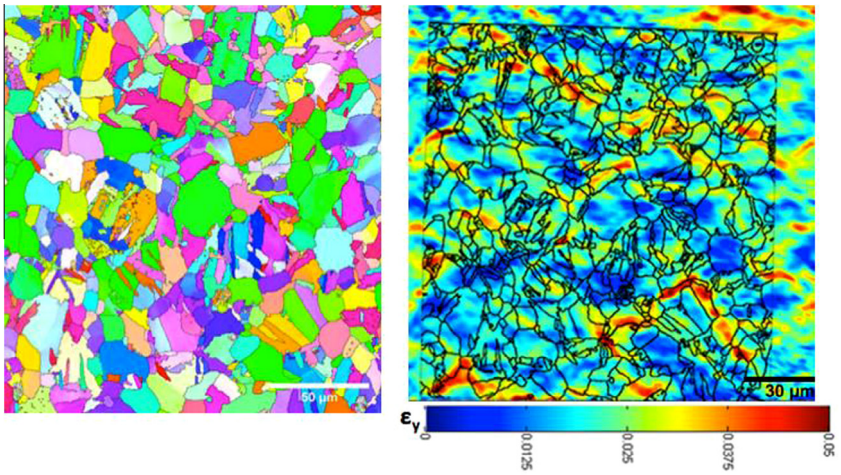


**Fig. 1.** Tensile strain field in a Titanium alloy microstructure as experimentally seen using micro-scale digital image correlation (Kammers and Daly, 2013, Prof. S. Daly, personal communication). Strains are seen to localize into shear bands within select grains.

the motion of surrounding particles. Using an integral form of the linear momentum balance equation, the method can directly model sharp displacement discontinuities (Agwai et al., 2011). This paper presents the first application of state-based peridynamic theory for crystal plasticity simulations. Current implementations of peridynamic state theory (Warren et al., 2009) employ explicit dynamic solution procedures that require small time steps for convergence. In this work, we employ a quasi-static implementation of the theory (Breitenfeld et al., 2014) and have extended it towards solving non-linear deformation problems. The solution procedure uses Newton–Raphson iterations similar to a non-linear finite element implementation. Thus, quasi-static peridynamics results can be quantitatively compared to conventional quasi-static crystal plasticity finite element simulations. Sections 2 and 3 of this paper provides the governing equations of the peridynamics theory and its numerical implementation. The crystal plasticity constitutive model is given in Section 4. In Section 5, we compare the method with crystal plasticity finite simulations and demonstrate the ability of peridynamics model to capture fine shear bands in grains. In the final section, conclusions and future work are discussed.

## 2. Peridynamics theory

In peridynamics theory, a material point $\boldsymbol{x}$ in the reference configuration $\mathcal{B}$ is assumed to interact with neighboring points $\boldsymbol{x}'$ (located within a finite radius $\delta$) along a bond defined by the vector $\boldsymbol{x}'-\boldsymbol{x}$. The position of particle $\boldsymbol{x}$ in the current configuration is denoted by $\boldsymbol{y}=\boldsymbol{x}+\boldsymbol{u}_{\boldsymbol{x}}$, where $\boldsymbol{u}_{\boldsymbol{x}}$ denotes the displacement of particle $\boldsymbol{x}$. The kinematics of peridynamics theory is shown in Fig. 2.

The equation of balance of linear momentum at time $t$ for the point $\boldsymbol{x}$ under quasi-static loading conditions is given by (Silling et al., 2007)

$$\begin{aligned}&\boldsymbol{L}(\boldsymbol{x})+\boldsymbol{b}(\boldsymbol{x})=0 \quad \forall x\in\mathcal{B},\\ &\boldsymbol{L}(\boldsymbol{x})=\int_{\mathcal{B}_x}\{\boldsymbol{T}[\boldsymbol{x}]\langle\boldsymbol{x}'-\boldsymbol{x}\rangle-\boldsymbol{T}[\boldsymbol{x}']\langle\boldsymbol{x}-\boldsymbol{x}'\rangle\}dV_{x'}\end{aligned} \tag{1}$$

where $\boldsymbol{b}$ is the body force, $\mathcal{B}_x$ is a spherical neighborhood of radius $\delta$ centered at $\boldsymbol{x}$ at time $t=0$. The term $\boldsymbol{T}[\boldsymbol{x}]\langle\boldsymbol{x}'-\boldsymbol{x}\rangle$ denotes the force (per unit volume squared) on material point $\boldsymbol{x}$ operating on the bond $\boldsymbol{x}'-\boldsymbol{x}$. The value of $\boldsymbol{T}$ can be obtained from the first Piola–Kirchhoff stress, $\boldsymbol{P}$, computed at point $\boldsymbol{x}$ from any conventional constitutive model (e.g. of the form $\boldsymbol{P}=\mathcal{F}(\boldsymbol{F})$, where $\boldsymbol{F}$ is the deformation gradient) as follows (Silling et al., 2007):

$$\boldsymbol{T}[\boldsymbol{x}]\langle\boldsymbol{x}'-\boldsymbol{x}\rangle=\omega\boldsymbol{P}\boldsymbol{K}^{-1}(\boldsymbol{x}'-\boldsymbol{x}) \tag{2}$$

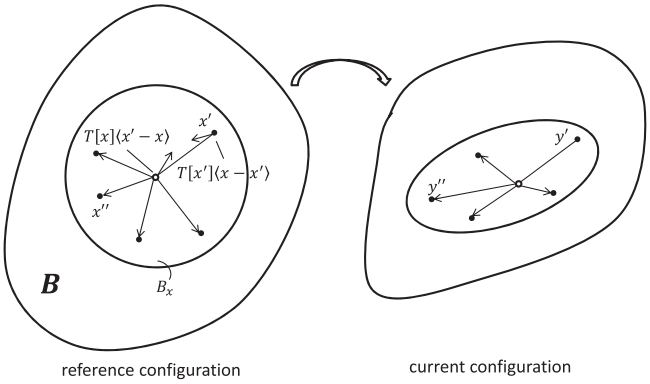


**Fig. 2.** Kinematics of peridynamics theory: Particle $\boldsymbol{x}$ is bonded to all particles within a region $\mathcal{B}_x$. Particle $\boldsymbol{x}$ maps to particle $\boldsymbol{y}$ in the deformed configuration. An averaged deformation gradient tensor can be defined that maps the bonds in the reference configuration to the deformed configuration. This quantity is used in the crystal plasticity constitutive model. The stresses obtained from the constitutive model can be mapped to bond force states $\boldsymbol{T}[\boldsymbol{x}]\langle\boldsymbol{x}'-\boldsymbol{x}\rangle$ in the reference configuration.

where, $\omega$ is an *influence function* defined at particle $\boldsymbol{x}$ which weights the contribution from each neighbor $\boldsymbol{x}'$ (for e.g. based upon the initial bond length $\omega=\hat{\omega}(|\boldsymbol{x}-\boldsymbol{x}'|)$) and $\boldsymbol{K}$ denotes a symmetric *shape tensor*, defined as

$$\boldsymbol{K}=\int_{\mathcal{B}_x}\omega(\boldsymbol{x}'-\boldsymbol{x})\otimes(\boldsymbol{x}'-\boldsymbol{x})dV_{x'} \tag{3}$$

The deformation gradient $\boldsymbol{F}$ (defined with respect to $\mathcal{B}$) at time $t$ as needed in the constitutive models can be computed from the deformation of bonds attached to material point $\boldsymbol{x}$ as follows (Silling et al., 2007):

$$\boldsymbol{F}=\left(\int_{\mathcal{B}_x}\omega(\boldsymbol{y}'-\boldsymbol{y})\otimes(\boldsymbol{x}'-\boldsymbol{x})dV_{x'}\right)\boldsymbol{K}^{-1} \tag{4}$$

The derivation of Eqs. (2) and (4) can be found in Section 18 of Silling et al. (2007) where it is also shown that these definitions ensure the balance of angular momentum.

## 3. Numerical implementation

By dividing the body $\mathcal{B}$ into numbers of cells, each represented by a particle, the integral expressions can be rewritten as a